Journal of Power Sources 246 (2014) 569–573

Contents lists available at ScienceDirect

Journal of Power Sources

journal homepage: www.elsevier.com/locate/jpowsour

Short communication

Effective enhancement of electrochemical performance for low-cost cathode material $Li_{1.231}Mn_{0.615}Ni_{0.154}O_2$ via a novel facile hydrothermal modification

Shi-Xuan Liao [a], Yan-Jun Zhong [a], Ben-He Zhong [a], Heng Liu [b], Xiaodong Guo [a,*]

[a] College of Chemical Engineering, Sichuan University, Chengdu 610065, China
[b] Material Science and Engineering Institute, Sichuan University, Chengdu 610064, China

HIGHLIGHTS

- A novel facile method is proposed to improve the electrochemical performance.
- The electrochemical performance of the cathode is successfully improved.
- The modified cathode exhibits enormous potential of energy storage.

ARTICLE INFO

Article history:
Received 21 June 2013
Received in revised form
25 July 2013
Accepted 1 August 2013
Available online 15 August 2013

Keywords:
Cathode material
Modification
Lithium manganese oxide
Lithium-ion batteries

ABSTRACT

A novel facile hydrothermal modification method is applied to improve the electrochemical performance of the low-cost cathode material $Li_{1.231}Mn_{0.615}Ni_{0.154}O_2$, which is primarily prepared by a solid-combustion approach. The material before and after modifying are characterized by energy dispersive spectrometer (EDS), powder X-ray diffraction (XRD), scanning electron microscopy (SEM), BET and high-resolution transmission electron microscopy (HRTEM). The samples are served as the cathode of lithium-ion batteries and investigated by galvanostatic experiments within a voltage range 2.0–4.8 V (*vs.* Li/Li^+). The results reveal that the electrochemical performance of the $Li_{1.231}Mn_{0.615}Ni_{0.154}O_2$ cathode electrode is prominently enhanced after modifying. The significantly improved electrochemical performance of the $Li_{1.231}Mn_{0.615}Ni_{0.154}O_2$ cathode is attributed largely to the modification of the surface microstructure and the crystallinity.

1. Introduction

Recently, layered Li_2MnO_3-stabilized cathode materials have become the promising cathode materials for lithium ion batteries. The capacity of the cathode is improved to 240–250 mAh g^{-1} by using layered Li_2MnO_3-stabilized cathode materials $xLi_2MnO_3\cdot(1-x)LiMn_{1/3}Ni_{1/3}Co_{1/3}O_2$ [1–3]. However, in large-scale applications, these materials are not so attractive due to the high cost, the toxicity and the impact on the environment of the cobalt. The cost of manganese is less than 1% of that of cobalt, and it is less toxic [4]. So the cost of the material can be drastically decreased by getting rid of using the cobalt and simultaneously increasing the manganese content. Here we select a low-cost composite $Li_{1.231}Mn_{0.615}Ni_{0.154}O_2$ (i.e., $0.6Li_2MnO_3\cdot0.4LiMn_{0.5}Ni_{0.5}O_2$) as the object material. Nevertheless, the Co-free Li_2MnO_3-stabilized composites with good electrochemical performance are scarcely obtained. Most of the researches focus on the structure, charge–discharge mechanism, but few reports about excellent electrochemical performance of these materials. S.-H. Kang et al. [5] reported an example $0.5Li_2MnO_3\cdot0.5LiMn_{0.5}Ni_{0.5}O_2$ with a low capacity of ~180 mA g^{-1} at 0.1 C and a poor rate capability; G. M. Koenig et al. [6] reported a $Li_{1.2}[Mn_{0.62}Ni_{0.38}]_{0.8}O_2$ electrode with a low capacity of 144 mAh g^{-1} at 1 C (here, 1 C corresponds to 200 mA g^{-1}).

Due to the poor electrochemical performance of this kind of material, a variety of approaches to improve the electrochemical performance have been proposed, such as adding a conductive substance (e.g., carbon) [7], metal doped (Al or Mg, etc.) approach [8,9], and surface modified with oxides (e.g., Al_2O_3) [10], fluorides [11], phosphates (e.g., $AlPO_4$) [12], and $LiMnPO_4$ [13] or $LiNiPO_4$ [14]. Even if sometimes the effects are great, whereas, these modification methods either are very complicated to operate or will result in degradation of theoretical capacity.

* Corresponding author. Tel.: +86 (0)28 85406702; fax: +86 (0)28 85405517.
E-mail address: xiaodong2009@scu.edu.cn (X. Guo).

0378-7753/$ – see front matter © 2013 Elsevier B.V. All rights reserved.
http://dx.doi.org/10.1016/j.jpowsour.2013.08.007

In the present work, we report for the first time the enhancement of electrochemical performance for the cathode material via a novel facile hydrothermal modification. The modified $Li_{1.231}Mn_{0.615}Ni_{0.154}O_2$ cathode electrode exhibits very excellent electrochemical performance: high rate performance, good cycle stability and high energy density of ~906 Wh kg^{-1} (20 mA g^{-1}, 2.0–4.8 V *vs.* Li/Li^+).

2. Experimental

The sample L0N ($Li_{1.231}Mn_{0.615}Ni_{0.154}O_2$) was prepared by a solid-combustion method. Appropriate amount of ethanol as dispersant, a certain quantity of sucrose as fuel, and stoichiometric amounts of Lithium salt ($LiNO_3$), nickel salt ($Ni(CH_3COO)_2{\cdot}4H_2O$) and manganese salt ($Mn(CH_3COO)_2{\cdot}4H_2O$) were mixed uniformly in milling vial for 10–15 min to obtain a solid–liquid rheological mixture, then ignited the mixture by a match to obtain an ash-like powder precursor. The obtained precursor was grounded and then calcined in air at 900 °C for 8 h.

The L0N was stirred in a hydrothermal synthesis container with appropriate amount of distilled water (e.g., in this work we use 20–50 g L0N, 600 mL H_2O) at 160–200 °C for normally 2–6 h. Then filter out the water to make powders contain moisture in small. The powders were dry at 120–150 °C for 1–2 h to obtain L1N.

3. Results and discussion

The Mn:Ni atomic ratios estimated by EDS are 8.1(8):2.1(2) for L0N, and 12.0(3):3.1(3) for L1N. In practice, the atomic ratios can hardly be signification of chemical composition of each samples, however, these demonstrate that the hydrothermal modification has little or no impact on the chemical ingredient of the as-prepared material. The crystal structure reflection patterns are collected with a scanning speed of 0.06° s^{-1} in the 2θ range from 10° to 70°, experimental data is displayed in Fig. 1. Nearly all of the reflections in XRD patterns of the samples (L0N, L1N) can be well indexed as the α-$NaFeO_2$ phase (hexagonal, *R*-3*m*). The excess monovalent lithium ions accommodate within the transition metal layers gives rise to the (020) reflection at around ~21° 2θ that highlighted by asterisk, which is characteristic of the integrated Li_2MnO_3-like component (monoclinic, *C*2/*m*) [15,16]. XRD result shows that the pair reflection peaks (006)/(012) and (018)/(110) for both L0N and L1N are well separated, and the intensity ratios $I_{(003)}/I_{(104)}$ and $[I_{(006)} + I_{(012)}]/I_{(101)}$ are 1.45 (1.78) and 0.344 (0.280) for L0N (L1N). The lattice parameters for L0N (L1N) are a = 2.85679 Å (2.85265 Å), c = 14.25158 Å (14.25903 Å) and V = 100.73 $Å^3$ (100.49 $Å^3$). As shown by the dashed line in Fig. 1(I) and (II) the reflection peak (110) experiences a slight 2θ position rightward shift. All the factors indicate that hydrothermal treatment more or less modifies the crystal structure of the integral solid solutions, which may well lead to the improvement of electrochemical performance [17]. Morphological examinations of the product powders are conducted by JSM-5900LV Scanning Electron Microscope. Fig. 2a and b shows that the average particle size decreases obviously from ~190 nm to ~110 nm after hydrothermal treatment. The specific surface area of L0N and L1N measured by N_2 absorption using the Brunauer–Emmett–Teller (BET) model are 6.45 and 9.28 $m^2\ g^{-1}$, respectively. According to previous studies [18,19], the decrease of the particle size and/or the increase of specific surface area are beneficial for rate performance. The effects of hydrothermal treatment on the particles, especially on the distribution characteristics (i.e., cumulative distribution and frequency distribution), are observed by the Laser Granulometric Analysis. The cumulative distribution curve (Fig. 2c) shifts to the left along the particle size axis after hydrothermal treatment, corresponding D_{10}, D_{50} and D_{90} decrease from 0.281, 1.740 and 12.197 μm to 0.242, 1.269 and 6.771 μm, respectively. Fig. 3 presents the microstructures of the oxide before and after modification by mean of TEM inspection (JEM-2100). It is evident that the sample L0N before modification has an amorphous-like phase with a thickness of around 3.5 nm from the observation of the edge of the block in the HRTEM image Fig. 3a. The amorphous-like phase without the occurrence of the clear interference fringe confirms the disordered structure in the surface layer instead of the single crystalline or polycrystalline feature. The disordered structure is disappeared after modification, and a better crystallinity of L1N than that of L0N is observed clearly. Furthermore, the lattice fringe spacing of ~4.27 Å indicating the presence of (020) planes at the edge of L0N block originating from the *C*2/*m* space group, which reveals a partial ordering surface [15,16,20]. However, the lattice fringes with a distance of ~4.7 Å ascribe to *C*2/*m* (001) planes and/or *R*-3*m* (003) planes provide evidence that the surface of L1N is mostly presents ordered planes rather than partial ordering ones. The modified surface microstructure and crystallinity after hydrothermal treatment are of benefit for Li+ intercalation/deintercalation between electrode and electrolyte, which may significantly improve the electrochemical performance of the cathode material (Fig. 4).

Electrochemical characterizations are carried out by assembling the samples into CR2032 coin cells in a glove box filled with argon, and the cells are estimated galvanostatically within an electrochemical window of 2.0 and 4.8 V (*vs.* Li/Li^+) at room temperature. All potentials presented in this paper were quoted versus the Li/Li^+ scale. The L0N electrode delivers a first discharge capacity of 161 mAh g^{-1} with coulombic efficiency of 64.4%. For L1N, the initial

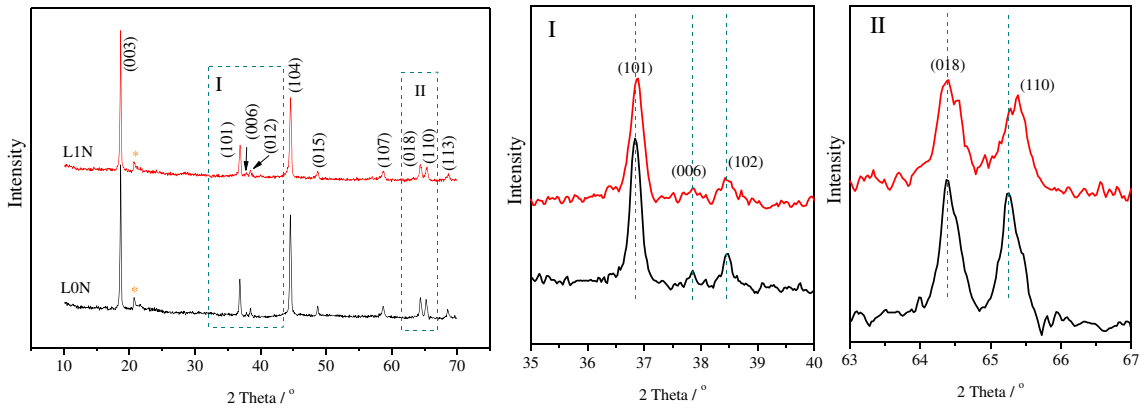

Fig. 1. XRD patterns for the samples; (I), (II) magnified area in the 35–40° region and the 63–67° region, respectively.

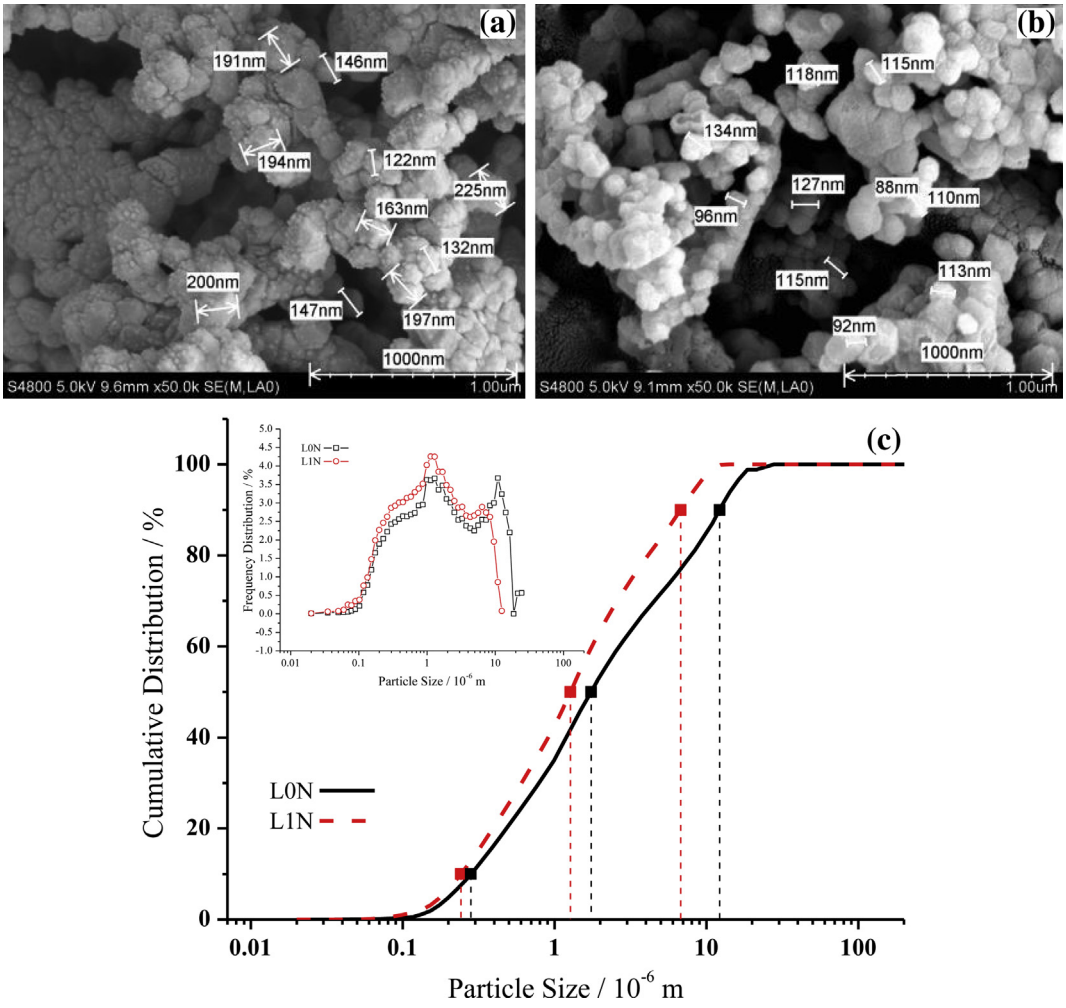

Fig. 2. SEM images of the composites, (a) for L0N, (b) for L1N, respectively. The SEM micrographs are prepared with the resolution of ×50,000; (c) particle distribution characteristics for the samples.

discharge capacity and coulombic efficiency are 261 mAh g^{-1} and 83.3%, respectively, superior to the L0N. The rate capabilities for L0N and L1N electrodes are depicted in Fig. 4a with the various test current rates 20, 40, 100, 200 mA g^{-1}, and finally in 20 mA g^{-1} in succession for L1N. The discharge capacities can reach 265 (258), 235 (223), 207 (163), and 186 (92) mAh g^{-1} for L1N (L0N) at the test current rates of 20, 40, 100, and 200 mA g^{-1}, respectively. The capacities of the first few cycles for both L0N and L1N are nearly the

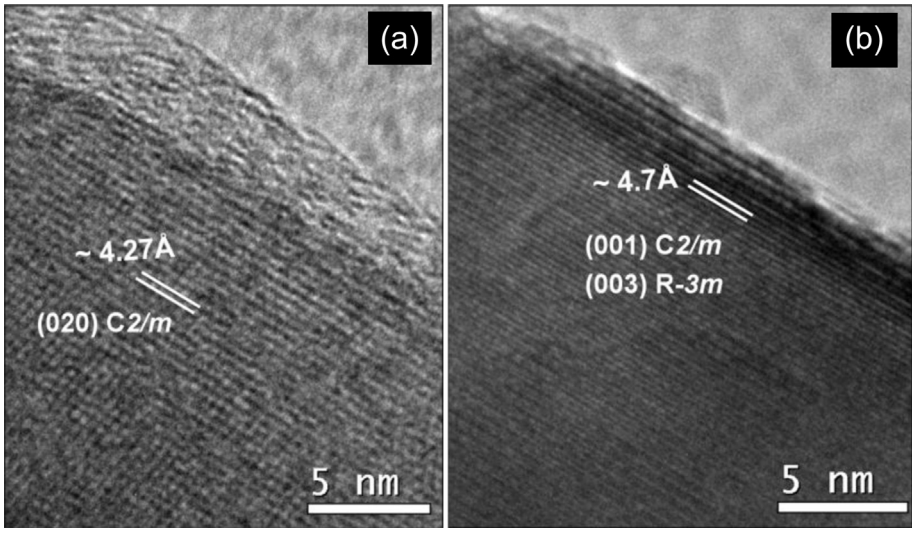

Fig. 3. High-resolution TEM (HRTEM) images (a) for L0N; (b) for L1N.

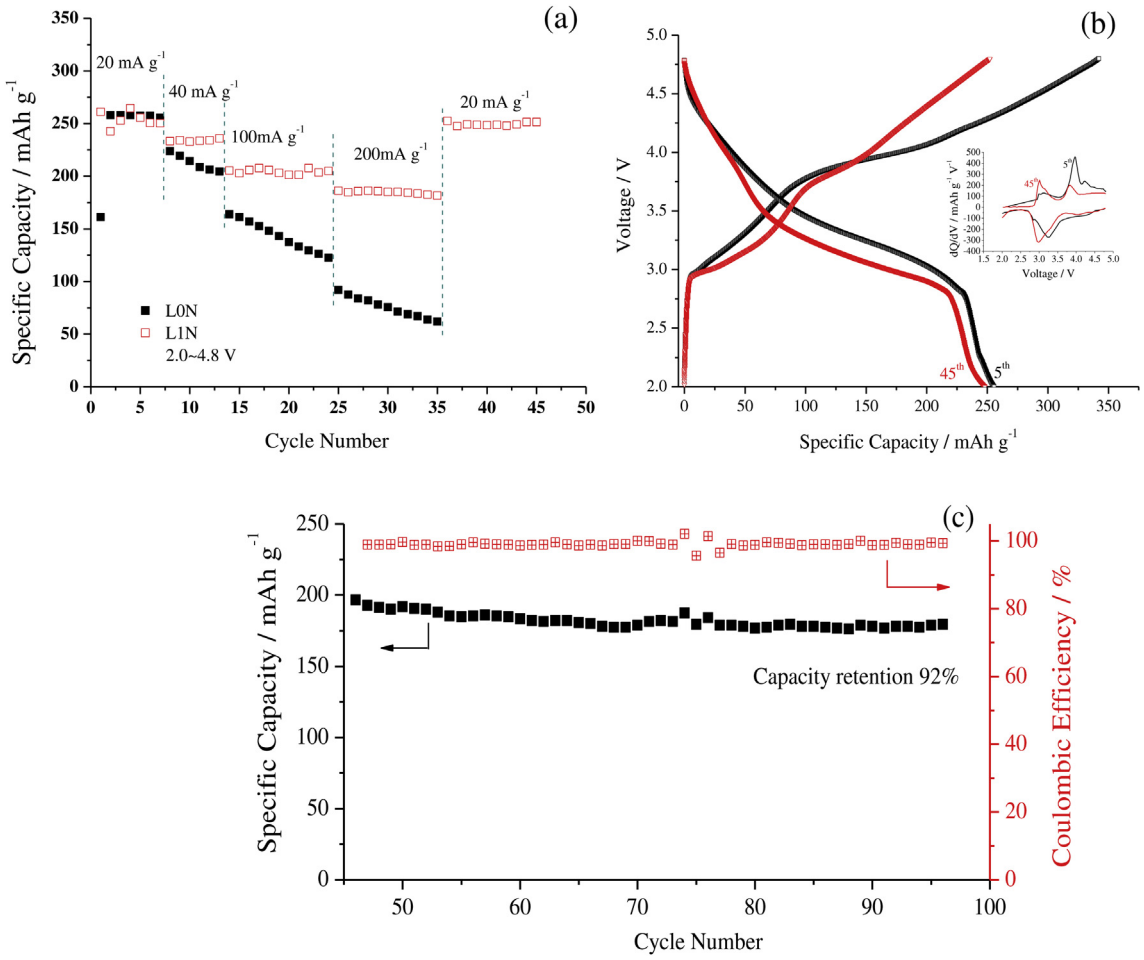

Fig. 4. (a) Rate performances of L0N and L1N; (b) charge–discharge curves of 5th and 45th with the inset corresponding differential capacity curves; (c) cycle stability for L1N at 100 mA g^{-1}.

same, which is due to the absence of additives and the similar electrode process at low charge–discharge current rate of 20 mA g^{-1}. Owing to the small particle size (~100 nm), with the increase of the test current rate, L1N electrode manifests significantly advantages on rate performances. In this work, we also found that the discharge capacities of each current rate for L1N are almost all more stable than L0N, and no evident degeneration is observed even at the high current rate cycles for L1N. Furthermore, the capacity of L1N can be recovered when the rate turns back to 20 mA g^{-1}. Although the charge–discharge (5th, 45th) curves and the corresponding dQ/dV–V curves have changed (Fig. 4b), the electrode is still a stable one (as observed during the 36th–45th cycles in Fig. 4a). Fig. 4c illustrates the cycle stability of the L1N that after rate capability examination. A good cycling stability is demonstrated with initial specific discharge capacity of 196 mAh g^{-1} and without noticeable capacity fading over 50 cycles. High coulombic efficiency near 100% is reached in 100 mA g^{-1} cycles, which reveals good reversibility of the material. It is particularly worth mentioning that L1N electrode delivers specific energy (E_m) of 906 (L0N, 882), 789 (L0N, 743), 674 (L0N, 494), and 570 (L0N, 222) Wh kg^{-1} at a constant current densities of 20, 40, 100, and 200 mA g^{-1}, respectively, which display enormous potential of energy storage (Here E_m is defined as the energy furnished from unit mass of active material with Li metal as anode [21], and the E_m can be determined by the equation: $E_m = \int P dt = \int\int I dV dt = \int Q(V) dV$).

4. Conclusion

The electrochemical performance of the cathode material $Li_{1.231}Mn_{0.615}Ni_{0.154}O_2$ is successfully enhanced by the hydrothermal modification. No impact on the chemical ingredient of the as-prepared material is observed. The surface microstructure and the crystallinity of the material have been ameliorated after the modification, the particle size decreased from ~190 nm to ~110 nm, and the specific surface area increased from 6.45 m^2 g^{-1} to 9.28 m^2 g^{-1}. All of these guarantee a better electrochemical performance for L1N than that of L0N. The discharge capacities of each current rate for L1N are almost all more stable than L0N. The specific energy density of L1N is approximately 2.6 times higher than that of L0N at the current density of 200 mA g^{-1}. Moreover, for the modified $Li_{1.231}Mn_{0.615}Ni_{0.154}O_2$ cathode electrode, a specific capacity of 180 mAh g^{-1} at 100 mA g^{-1} after 50 cycles is got, which means 92% of initial capacity is remained after the cyclings. In conclusion, we present a novel facile technique to improve the electrochemical performance of the Co-free Li-rich and Mn-rich oxide cathode material $Li_{1.231}Mn_{0.615}Ni_{0.154}O_2$. Maybe the modification technique is also attractive for some other cathode materials due to the following advantages: (1) It is simple to operate; (2) It has no negative influences on theoretical capacity, which causes by the electrochemical inactive additives; (3) It is capable of mass modifying materials, which is superior to the extremely difficult

and small-scale hydrothermal synthesis approach in comprehensive assessment.

Acknowledgments

This work was supported by the Sichuan University Funds for Young Scientists (No. 2011SCU11081), and the Research Fund for the Doctoral Program of Higher Education, the Ministry of Education (No. 20120181120103). The Analysis and Test Center of Sichuan University also supported this study.

References

[1] H. Koga, L. Croguennec, P. Mannessiez, M. Ménétrier, F. Weill, L. Bourgeois, M. Duttine, E. Suard, C. Delmas, J. Phys. Chem. C 116 (2012) 13497.
[2] C.S. Johnson, N. Li, C. Lefief, J.T. Vaghey, M.M. Thackeray, Chem. Mater. 20 (2008) 6095.
[3] M.M. Thackeray, S.-H. Kang, C.S. Johnson, J.T. Vaughey, R. Benedek, S.A. Hackney, J. Mater. Chem. 17 (2007) 3112.
[4] A.R. Armstrong, P.G. Bruce, Nature 381 (1996) 499.
[5] S.-H. Kang, P. Kempgens, S. Greenbaum, A.J. Kropf, K. Amine, M.M. Thackeray, J. Mater. Chem. 17 (2007) 2069.
[6] G.M. Koenig Jr., I. Belharouak, H. Deng, Y.-K. Sun, K. Amine, Chem. Mater. 23 (2011) 1954.
[7] J. Kim, B. Kim, J. Lee, J. Cho, B. Park, J. Power Sources 139 (2005) 289.
[8] C.J. Jafta, K.I. Ozoemena, M.K. Mathe, W.D. Roos, Electrochim. Acta 85 (2012) 411.
[9] A. Boulineau, L. Simonin, J.-F. Colin, E. Canevet, L. Daniel, S. Patoux, Chem. Mater. 24 (2012) 3558.
[10] J. Cho, Y.J. Kim, T.-J. Kim, B. Park, Chem. Mater. 13 (2001) 18.
[11] Y.K. Sun, M.J. Lee, C.S. Yoon, J. Hassoun, K. Amine, B. Scrosati, Adv. Mater. 24 (2012) 1192.
[12] Q.Y. Wang, J. Liu, A.V. Murugan, A. Manthiram, J. Mater. Chem. 19 (2009) 4965.
[13] Q.Q. Qiao, H.Z. Zhang, G.R. Li, S.H. Ye, C.W. Wang, X.P. Gao, J. Mater. Chem. A 1 (2013) 5262.
[14] S.-H. Kang, M.M. Thackeray, Electrochem. Commun. 11 (2009) 748.
[15] D. Luo, G. Li, X. Guan, C. Yu, J. Zheng, X. Zhang, L. Li, J. Mater. Chem. A 1 (2013) 1220.
[16] J. Bréger, M. Jiang, N. Dupré, Y.S. Meng, Y. Shao-Horn, G. Ceder, C.P. Grey, J. Solid State Chem. 178 (2005) 2575.
[17] K.M. Shaju, G.V.S. Rao, B.V.R. Chowdari, Electrochim. Acta 48 (2002) 145.
[18] Y. Ren, A.R. Armstrong, F. Jiao, P.G. Bruce, J. Am. Chem. Soc. 132 (2010) 996.
[19] K.T. Lee, J. Cho, Nano Today 6 (2011) 28.
[20] J.-S. Kim, C.S. Johnson, J.T. Vaughey, M.M. Thackeray, Chem. Mater. 16 (2004) 1996.
[21] Z. Zhu, H. Yan, D. Zhang, W. Li, Q. Lu, J. Power Sources 224 (2013) 19.